01 Jan 2020

A New Type of Crumb Rubber Asphalt Mixture: A Dry Process Design and Performance Evaluation

Feng Ma

Jiasheng Dai

Zhen Fu

Jenny Liu
Missouri University of Science and Technology, jennyliu@mst.edu

et. al. For a complete list of authors, see https://scholarsmine.mst.edu/civarc_enveng_facwork/1799

Recommended Citation

F. Ma et al., "A New Type of Crumb Rubber Asphalt Mixture: A Dry Process Design and Performance Evaluation," *Applied Sciences (Switzerland)*, vol. 10, no. 1, MDPI AG, Jan 2020.
The definitive version is available at https://doi.org/10.3390/app10010372

applied sciences

MDPI

Article

A New Type of Crumb Rubber Asphalt Mixture: A Dry Process Design and Performance Evaluation

Feng Ma [1], Jiasheng Dai [1], Zhen Fu [2,*], Jenny Liu [3], Wenhao Dong [1] and Zhen Huang [1]

[1] Key Laboratory for Special Area Highway Engineering of Ministry of Education, Chang'an University, Xi'an 710064, China; mafeng@chd.edu.cn (F.M.); daijiasheng@163.com (J.D.); dongwenhao@chd.edu.cn (W.D.); 2018221146@chd.edu.cn (Z.H.)

[2] School of Material and Science Engineering, Chang'an University, Xi'an 710064, China

[3] Department of Civil, Architectural and Environmental Engineering, Missouri University of Science and Technology, Rolla, MO 65409, USA; jennyliu@mst.edu

* Correspondence: zhenfu@chd.edu.cn; Tel.: +86-029-8233-4823

Received: 27 November 2019; Accepted: 30 December 2019; Published: 3 January 2020

Abstract: To obtain a crumb rubber asphalt mixture with excellent performance, this study combined trans-polyoctenamer rubber (TOR), crumb rubber, and other additives to establish a new type of crumb rubber (CRT). The objective of this study was to design and evaluate the road performance of the new type of crumb rubber asphalt mixture (CRTAM) with a skeleton dense texture through a dry process. First, the skeleton intrusion compact volume method was used to optimize the grading of coarse and fine aggregates, and the design of the CRTAM gradation was carried out through the same and unequal volume replacement grading method. Then, three types of road performance were analyzed: high-temperature stability, low-temperature crack resistance, and water stability. The results showed that 2% and 2.5% CRT met a low-temperature index with equal volume substitution, and the six gradations obtained by unequal volume replacement with 2% CRT complied with the requirements of a skeleton dense texture. When the substitution ratio was 1.5 and 0.5, the high-temperature performance was better. In addition, when the substitution ratio was 0.5, the flexural strain energy density was the highest and the low-temperature performance was the best. Including considerations of economic benefits, it is recommended that the CRT content be 2% and the substitution ratio be 0.5.

Keywords: asphalt mixture; dry process design; crumb rubber; trans-polyoctenamer rubber; road performance

1. Introduction

Globally, ever-increasing traffic and growing axle loads have urged engineers and practitioners to use and adopt unconventional asphalt materials for the improvement of pavement performance [1–4]. Crumb rubber (CR), which is used as a modifier for asphalt, has been proven to endow asphalt with improved properties, i.e., better rutting resistance, fatigue resistance, water stability, antireflective cracking ability, and decreased road costs [5–7]. Meanwhile, CR also provides an effective approach to solving the "black pollution" caused by the accumulation of waste tires [8]. Therefore, crumb rubber-modified asphalt (CRMA) and crumb rubber asphalt mixtures (CRAMs) are very popular in engineering and research.

In recent years, many efforts have been made in terms of the manufacturing processes, various properties, and influences of rubber properties and asphalt. Bressi et al. [9] showed that the science and technology of the recycling of waste tire rubber is developing rapidly all over the world. It was found that the viscosity of CRMA will increase no matter what kind of rubber addition method is used.

Recycled tire rubber also had a significant effect on the rheology of the asphalt binder, showing higher rutting resistance. Vazquez et al. [10] found that the use of CR as a modifier of asphalt (CRMB) can improve the pavement characteristics that are added by the wet process. Furthermore, gap-graded CRAMs can be used to fight noise pollution. Licitra et al. [11] used a new method to investigate and model the acoustic aging of several rubberized road surfaces produced in accordance with the wet process, which were laid on three different sites. On the other hand, CR contributes to layer endurance during its service life. Therefore, reclaimed asphalt pavement (RAP) binder is often used with CRMA to make up for the adverse effects of RAP binder on the fatigue performance of mixtures [12,13]. Some studies have further shown that this combination can provide more advantages in reducing material costs and solving waste disposal issues [14–16].

However, CRAMs exhibit problems of aging, crumb rubber swelling, storage stability, and compaction [17,18]. Therefore, CR is modified and activated by preswelling agents, desulfurization, and plasticization to improve the compatibility of granular green rubber with asphalt [19,20]. Yu et al. [21] found that CRMA activated by microwaves exhibited minor temperature-sensitive behavior and storage stability, improved viscoelasticity, and high ductility at 5 °C. In addition, reactive additives such as polyphosphoric acid [22], crosslinking agents [23], and trans-polyoctenamer rubber (TOR)-reactive modifier [24] have provided a new approach to improving the performance of CRMA. Among the abovementioned additives, TOR is a polymeric reactive rubber with a high amount of unsaturated bonds in its molecules, showing high reactivity [23]. It is obtained through the polymerization of cyclooctene monomer through a metathesis reaction, in which cyclooctene monomer is synthesized from 1,3-butadiene and 1,5-cyclooctadiene [25]. Liang et al. [24,26] found that TOR-activated CRMA improved low-temperature creep behavior, showed more obvious hardening effects after aging, and improved CRMA storage stability. Double bonds in TOR participate in chemical reactions and are beneficial for stability. Liu et al. [27] showed a complex chemical reaction between TOR and CRMA at a microscopic level, which changed the rheological properties of CRAM and contributed to its storage stability. It has been noted that TOR can promote a chemical reaction between CR and virgin asphalt, which provides CR and CRMA with the characteristics of preventing cracks, waterproofing, noise reduction, simple construction technology, flexibility, good construction workability, and favorable heat storage stability [6,28,29].

The problem of expansion after the action of asphalt and CR is also one of the problems affecting the performance of CRAMs. The methods of producing CRAMs are mainly wet and dry processes [5,30]. In the wet process, CR is added to a traditional sharpener and mixed into virgin asphalt with the characteristics of modified asphalt, which can be used as a binder for asphalt mixtures. In the dry process, CR with relatively coarse particles is added to the aggregate and then sprayed into the hot asphalt to form asphalt mixtures [31,32]. Compared to the wet process, the dry process is simpler, does not require special equipment, and can consume more used tires [33,34]. López-Moro et al. [35] found from a microscopic point of view that the addition of CR to the dry process increases the hardness of the asphalt, improves the rutting resistance, and changes the shape and porosity of the CR due to the interaction between rubber and asphalt. The optimum size (<200 μm) for rubber particles in the dry mixing process was obtained. Gawel et al. [36] found that CR can expand to three times its original size during rubber–asphalt interactions and may resist subsequent compaction. This expansion effect prevents the mixture from reaching its target density, leading to premature failure, such as cracking and loosening. Moreover, many studies have proven that skeleton dense texture can reserve enough space to accommodate the volume of CR expansion, which prevents CR from interfering with asphalt mixture gradation [37–39]. In addition, skeleton dense texture lowers the asphalt dosage, and the asphalt dosage is saved compared to a virgin asphalt mixture. The oil savings are generally 0.3–0.6% [34,35].

Although previous studies have demonstrated that the addition of TOR could improve the performance of CRMA and become a viable option in asphalt pavement, it has also been proven that the preparation of CRAMs through the dry process could better solve the expansion problem of CR. However, the combination of TOR activator and the dry process has not been studied. In order to

obtain a CRAM with excellent performance, a new direction for research and the application of CRAMs was developed. On the basis of TOR-activated CR, a new type of CR was developed, and a new type of CRAM with a skeleton dense texture was designed through the dry process (abbreviated as CRTAM). First, using the traditional design method, optimized gradation and the compact gradation design method were adopted to make the CR play a role in the asphalt modification and at the same time fill the aggregate. In addition, road performance, i.e., high-temperature stability, low-temperature crack resistance, and water stability, was analyzed through experiments. It is anticipated that the research results of this study will benefit the engineering practices of dry-processed CRTAM and promote its wider application.

2. Materials and Research Content

2.1. Materials

2.1.1. Asphalt

In this study, certain technical properties of base asphalt were evaluated by following the Chinese standard "Technical Specifications for Highway Asphalt Pavement Construction" (JTJ F40). The test results are listed in Table 1.

Table 1. Virgin asphalt binder properties.

Items		Units	Test Results	Specification Limits
Penetration (25 °C, 100 g, 5 s)		0.1 m	88.2	80–100
Ductility (5 cm/min, 15 °C)		cm	128.8	≥100
Ductility (5 cm/min, 10 °C)		cm	34.6	≥20
Softening point (righ and ball method)		°C	46.5	≥45
Flash point (COC)		°C	297	≥245
Wax content (distillation method)		%	1.9	≤2.2
Density (15 °C)		g/cm^3	0.99	—
Solubility (trichloroethylene)		%	99.6	≥99.5
The thin film oven test (TFOT) (163 °C, 5 h)	Residual penetration ratio	%	73.6	≥57
	Ductility (5 cm/min, 15 °C)	cm	>100	≥20
	Ductility (5 cm/min, 10 °C)	cm	8.26	≥8

2.1.2. Aggregate and Filler

Limestone was used as the aggregate of the asphalt mixture. When measuring various performance indexes of aggregates, it was considered that a particle size of 2.36 mm and above was the coarse part of the aggregate and a particle size below 2.36 mm was the fine part of the aggregate. Limestone powder was selected as a filler for the asphalt mixture, in which no moisture or agglomeration was observed. The method in "Testing Regulations for Highway Engineering Aggregates" (JTG E42-2005) can be referred to for a determination of aggregate technical indicators. The properties of the coarse aggregate and filler are listed in Table 2. The densities of the coarser part (2.36 mm–13.2 mm) and finer part (0.075 mm–1.18 mm) are listed in Table 3.

Table 2. Properties of coarse aggregate and filler.

Materials	Properties	Units	Specification Limits		Test Result
			Surface Layer	Other Layers	
Coarse aggregate	Stone crushing value	%	≥26	≥28	12.5
	Los Angeles wear loss	%	≥28	≥30	16.0
	Apparent relative density	%	≥2.60	≥2.50	2.8
	Water absorption rate	%	≥2.0	≥3.0	0.90
	Rugged	%	≥12	≥12	6.0
	Needle-like particle content (mixture)	%	≥15	≥18	6.8
	Particle size greater than 9.5 mm		≥12	≥15	
	Particle size less than 9.5 mm		≥18	≥20	
	Particle content <0.075 mm through washing method	%	≥1	≥1	4.2
	Soft stone content	%	≥3	≥5	8.8
Filler	Apparent density	g/cm3	≥2.5		2.724
	Particle size range <0.6 mm	%	100		100
	<0.15 mm		90–100		99.8
	<0.075 mm		80–100		85.3
	Hydrophilic coefficient	—	<1		0.58
	Water content	%	≤1		0.1
	Plasticity index	—	<4		3.3

Table 3. Coarse aggregate and finer aggregate density.

Density	Aggregate Specification (mm)								
	13.2	9.5	4.75	2.36	1.18	0.6	0.3	0.15	0.075
Apparent relative density	2.896	2.940	2.807	2.841	—	—	—	—	—
Bulk volume relative density	2.779	2.870	2.773	2.757	—	—	—	—	—
Apparent relative density	—	—	—	—	2.822	2.791	2.796	2.834	2.805

2.1.3. Preparation of a New Type of Crumb Rubber (CRT)

Since ordinary crumb rubber material has poor compatibility with asphalt, its elastic advantage is not fully exerted. Thus, its effect on road performance improvement is limited. CRT is a new rubber powder material made up of 40-mesh crumb rubber, TOR coupling agent, and some other materials. The advantage of this material is that it is developed through the dry process, which can solve the problems in the performance of the asphalt mixture due to the large content of CR. The properties of CRT and CR are listed in Table 4. The gradation of CRT is listed in Table 5.

Table 4. Performance of CRT and crumb rubber (CR).

Materials	Properties	Units	Specification Limits	Test Results
CRT	Relative density	g/cm^3	—	1.21
	Water content	%	<1.0	0.53
	Metal content	%	<0.01	0.004
	Fiber content	%	<1.0	0.003
CR	Relative density	g/cm^3	1.10–1.30	1.20
	Water content	%	<1.0	0.56
	Metal content	%	<0.05	0.016
	Fiber content	%	<1.0	0.0
	Ash content	%	≤8	3.9
	Acetone extract	%	≤22	14
	Carbon black content	%	≥28	40

Table 5. The gradation of CRT.

Sieve Size (mm)	2.36	1.18	0.6	0.3	0.15	0.075
Percentage passing (%)	100	90.34	70.23	38.66	10.3	1.23

2.2. Research Contents

In order to improve research on the gradation of CRTAM pavement, the optimization design of CRTAM gradation was carried out through laboratory tests, and road performance was comprehensively analyzed. This provided reliable technical support for the research and promotion of the large-area use of rubber and virgin asphalt pavement. For this paper, CRTMA was produced through the dry process. Figure 1 illustrates the complete research framework.

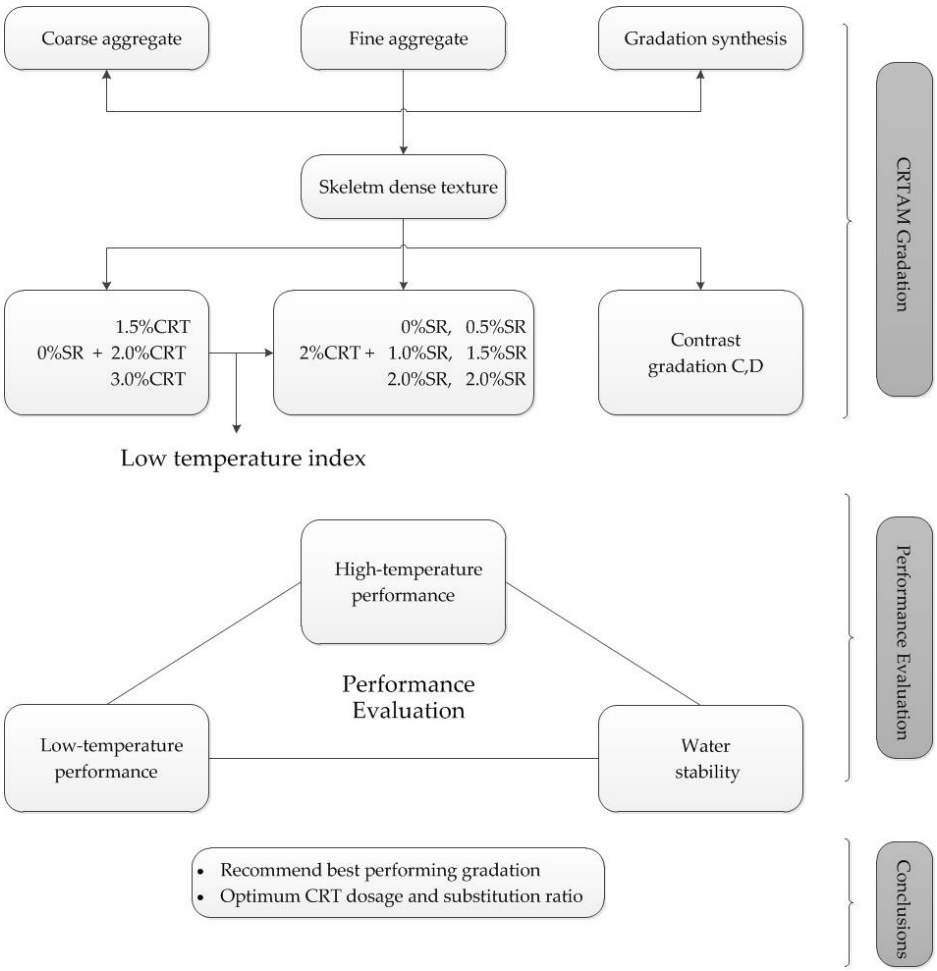

Figure 1. Research framework.

3. Gradation Design

3.1. Coarse and Fine Aggregate Design

3.1.1. Division of Coarse and Fine Aggregates

According to the definition of a coarse aggregate, the key to dividing the boundary is to find the minimum particle size that acts as a skeleton. It is not suitable to use a single sieve hole of 4.75 mm or 2.36 mm. Therefore, a single particle crush test was performed on aggregates with a particle size of

19 mm to 2.36 mm, and the crushed aggregate particles were separately sieved. The test results are shown in Figure 2.

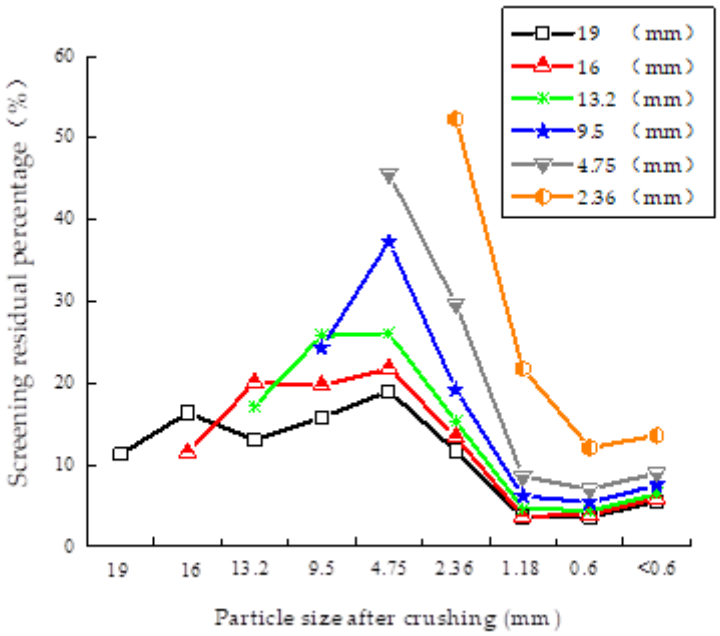

Figure 2. Particle size distribution after crushing each particle size.

According to the test results, when the original particle size was larger than 4.75 mm, the peak occurred generally at 4.75 mm after the crushing. A large number of 4.75-mm particle size particles appeared after the crushing. The aggregate reconstituted the new structure after breaking, mainly due to the 4.75-mm particle size aggregate. It can be assumed that 4.75 mm was the main supporting part of the skeleton structure after the crushing, so that the mixture had a higher bearing capacity. Therefore, the cut-off points of the coarse and fine particle sizes used in this study were 2.36 mm or 4.75 mm.

3.1.2. Coarse Aggregate Design

Using a combination of experience and theory and referring to the Dinger–Funk equation and the idea of the gradation fractal theory of concrete and soil particles, a mathematical model of sieve-hole throughput at different levels of coarse aggregates was calculated, as in Equation (1). Gradation 1 was carried out according to 2.36 mm as the dividing point of the coarse and fine aggregates, and gradation 2 was carried out according to 4.75 mm as the dividing point of the coarse and fine aggregates. Gradations 1 and 2 were calculated according to Equation (1), and the density and the gap ratio were measured in the three states of compaction, selecting, and loosening. The density could be taken as 1.03 times the bulk density, and the results are listed in Table 6. Equation (1) is

$$\frac{P(Di)}{P(Di\ +\ 1)} = \frac{D_i^x - D_{\min}^x}{D_{\max}^x - D_{\min}^x} \times 100\%, \tag{1}$$

where $P(Di)$ = the pass rate (%) of the mesh with particle size Di; $P(Di\ +\ 1)$ = the pass rate (%) of the mesh with particle size $Di\ +\ 1$; $x = (\lg D_{\max} - \lg Di)/\lg Di$; D_{max} = the maximum particle size of the coarse aggregate; and $D_{\min}$ = the minimum particle size of the coarse aggregate.

Table 6. Calculation results of the sieve pass rate of the coarse aggregate.

Gradation Types	Particle Size Range (mm)	Proportion (%)	Density (kg/m^3)			Air Void (%)		
			Tamping State	Select Tight State	Loose State	Tamping State	Select Tight State	Loose State
Gradation 1	16–13.2	10.7	1.683	1.573	1.527	39.858	43.809	45.444
	13.2–9.5	28.4						
	9.5–4.75	48.1						
	4.74–2.36	12.8						
Gradation 2	16–13.2	16.5	1.696	1.604	1.557	39.675	42.941	44.601
	13.2–9.5	38.8						
	9.5–4.75	44.8						

3.1.3. Fine Aggregate Design

In order to form an embedded structure between the grading particles and ensure that the gap ratio was small enough to improve the overall stability of the mixture, the grading filling theory was used to design the fine aggregate ratios of coarse aggregate gradations 1 and 2. The method of finding the best ratio for the lowest porosity was refined.

Here, take the class I filling in gradation 1 as an example. The aggregate of 2.36–1.18 mm and 1.18–0.6 mm was given a total weight of 5 kg in accordance with the proportions in Table 7, and the aggregate was evenly mixed as the test material. The test results are shown in Table 7. Figure 3 is a graph of the variation in the air void proportional to the different compositions of the aggregate (wt %).

Table 7. Class I filling test results.

Projects	Units	Different Composition Ratios of 2.36–1.18-mm and 1.18–0.6-mm Aggregates								
		10:0	9:1	8:2	7:3	6.5:3.5	6:4	5.5:4.5	5:5	4:6
Aggregate quality	g	1520	1540.5	1562	1572	1575.5	1576.5	1576.6	1569.5	1541.5
Tight density	g/cm^3	1.462	1.481	1.502	1.512	1.515	1.516	1.516	1.509	1.482
Apparent density	g/cm^3	2.822	2.819	2.816	2.813	2.811	2.810	2.808	2.806	2.803
Air void	%	48.209	47.452	46.660	46.259	46.109	46.045	46.016	46.226	47.127

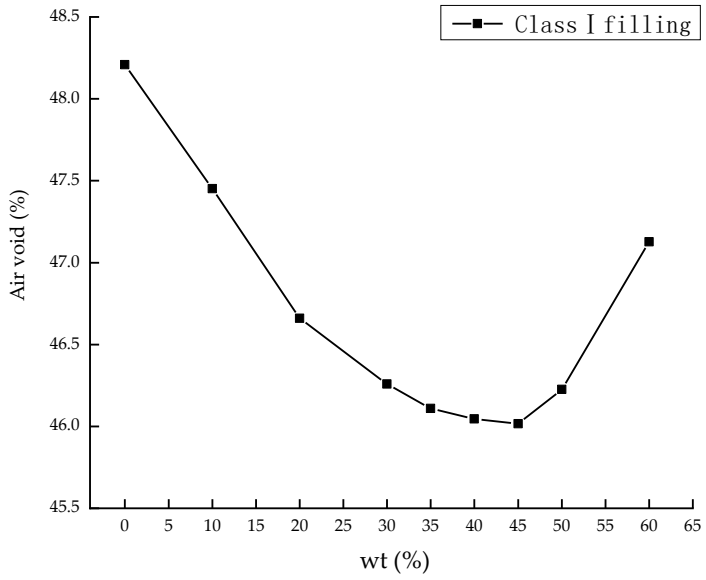

Figure 3. Air void at different ratios of 2.36–1.18 mm and 1.18–0.6 mm.

From the peak fitting analysis in Figure 3, we can get an arrangement ratio between 2.36–1.18 mm and 1.18–0.6 mm of 55:45. The skeletal structure formed by the aggregates of two particle sizes under this gradation was the densest, and the air void was 46.016%. Then, the class II filling was carried out with the results of the class I filling, and the subsequent fillings were carried out by superposition.

Therefore, the class I–IV fillings and class I–V fillings were performed on gradation 1 and gradation 2, respectively, according to the division boundaries of the coarse and fine aggregates. The results of the two-stage grading and filling are shown in Figure 4. According to the relationship between the void ratio and the proportion of the filling for each class, the optimum ratio value under the filling of the level was obtained by peak fitting. The grading compositions are listed in Table 8.

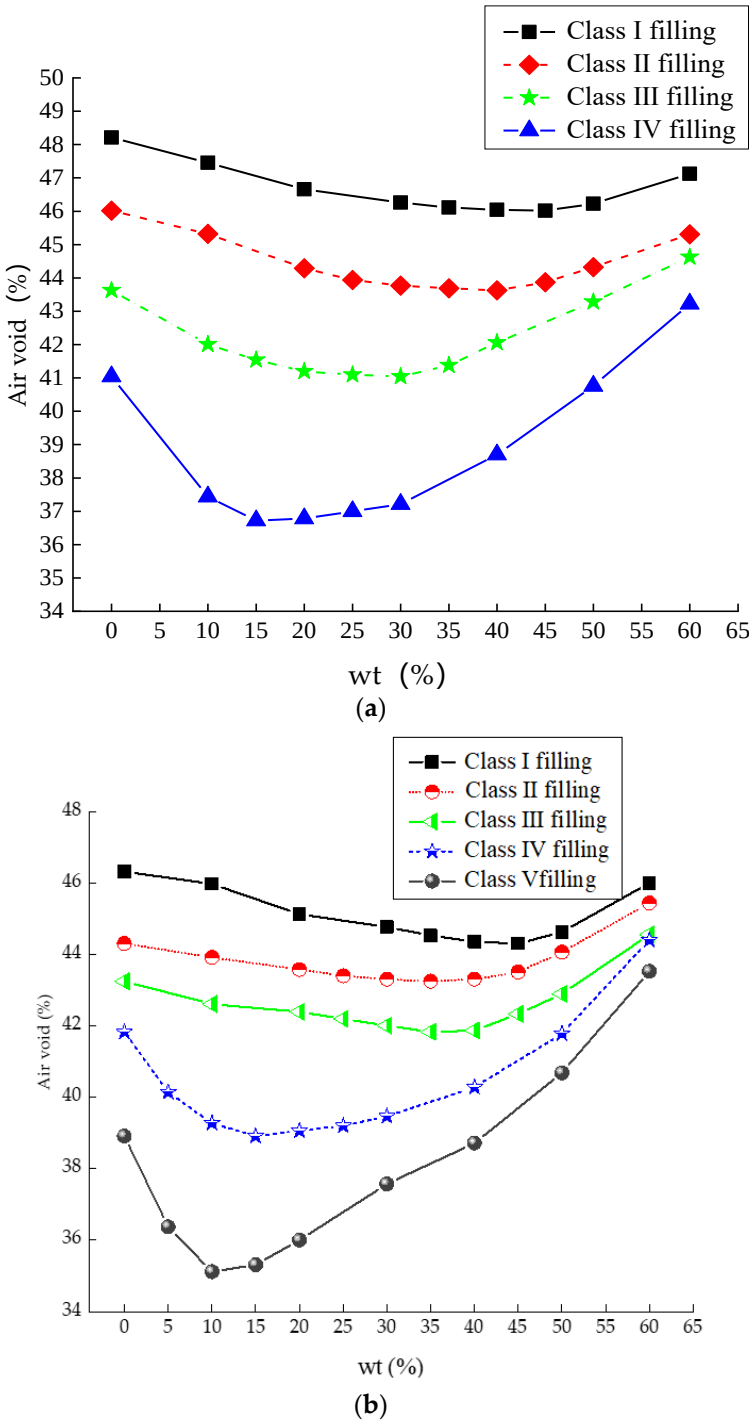

Figure 4. Air void variations with secondary particle size fractions: (**a**) gradation 1; (**b**) gradation 2.

Table 8. Fine aggregate grading compositions.

Gradation Types	Particle Size Range (mm)	Proportion (%)	Synthetic Apparent Density (g/cm^3)	Tight Density (g/cm^3)	Air Void (%)
Gradation 1	2.36–1.18	19.64	2.811	1.779	36.724
	1.18–0.6	16.07			
	0.6–0.3	23.80			
	0.3–0.15	25.50			
	0.15–0.075	15.00			
Gradation 2	4.75–2.36	17.78	2.813	1.825	35.118
	2.36–1.18	14.54			
	1.18–0.6	17.40			
	0.6–0.3	26.78			
	0.3–0.15	13.50			
	0.15–0.075	10.00			

3.2. Gradation Synthesis

3.2.1. Gradation Design

In the absence of mineral powder and binder, according to the step-by-step filling theory, in order to minimize the gap of the skeleton structure formed between the coarse aggregates and to avoid its expansion through the fine aggregate, the secondary skeleton dense structure should completely fill the main skeleton's gap. Therefore, the composition design of CRT should adopt the volume method, and some improvement measures should be made on the basis of the coarse aggregate void-filling (CAVF) method. The skeleton intrusion compact volume method was proposed. The calculation process is as follows:

$$q_c + q_f + q_p = 100\%, \tag{2}$$

$$\frac{q_c}{100\rho_{sc}}(\mathrm{VCA} - \mathrm{V_{VS}}) = \frac{q_p}{\rho_{tp}} + \frac{q_f}{\rho_{tf}} + \frac{q_a}{\rho_a} + \frac{q_r}{\rho_{tr}}, \tag{3}$$

$$\frac{q_a}{100\rho_a} = (\mathrm{VMA} - \mathrm{V_{VS}}) \times \frac{q_c}{100\rho_{sc}}, \tag{4}$$

where q_c, q_f , q_p , q_r, and q_a are the mass fractions of the coarse aggregate, fine aggregate, filler, CR, and asphalt, respectively; ρ_{sc}, ρ_{tp}, ρ_{tf}, ρ_a, and ρ_{tr} are the apparent densities of the coarse aggregate, filler, fine aggregate, asphalt, and CR, respectively; VCA = the air void; $\mathrm{V_{VS}}$ = the objective void; and VMA = the void in the mineral aggregate.

In the design, when CR is not incorporated, if $\mathrm{V_{VS}}$, VMA, and q_p are determined, other parameters can be calculated. VVS was set to 4%, VMA was set to 15%, and gradation 1 was taken as 5%. It can be seen from Table 8 that the VCA of fine aggregate gradation 1 was slightly larger than that of gradation 2. In order to better fill the coarser fine aggregate, the gradation 2 filler content was smaller than that of gradation 1. At the same time, considering that the dry process asphalt mixture in the later stage adopted a skeleton dense gradation, a gradation 2 of 4% was considered to be comprehensive.

For the calculation, let X be the percentage of coarse aggregate, Y be the percentage of fine aggregate, Z be the asphalt–aggregate ratio, and the other parameters be as listed in Table 2, Table 6, and Table 8. The results are listed in Table 9, and the synthetic gradations are listed in Table 10. The proportion of coarse aggregates was generally between 65% and 75%, and the loose state of gradation 1 did not meet the requirement.

Table 9. Calculation results under different filling methods.

Gradation	State	*X* (%)	*Y* (%)	*Z* (%)
1	Tamping state	70.8	24.2	4.58
	Select tight state	66.1	28.9	4.58
	Loose state	64.2	30.8	4.58
2	Tamping state	71.1	24.9	4.56
	Select tight state	67.2	28.8	4.56
	Loose state	65.2	30.8	4.56

Table 10. Gradation under different filling methods.

Gradation	Particle Size (mm)	16	13.2	9.5	4.75	2.36	1.18	0.6	0.3	0.15	0.075
1	Tamping state	100.00	92.42	72.34	38.28	29.20	24.45	20.56	14.80	8.63	5.00
	Select tight state	100.00	92.92	74.18	42.38	33.90	28.23	23.58	16.70	9.34	5.00
	Loose state	100.00	93.13	74.92	44.03	35.80	29.75	24.80	17.47	9.62	5.00
2	Tamping state	100.00	88.30	60.75	28.90	24.47	20.85	16.52	9.85	6.49	4.00
	Select tight state	100.00	88.95	62.90	32.80	27.68	23.49	18.48	10.77	6.88	4.00
	Loose state	100.00	89.27	64.01	34.80	29.32	24.85	19.48	11.24	7.08	4.00

3.2.2. Aggregate Grading Optimization

The coarse aggregate ratio R_{CA} was used to evaluate the rationality of the composition between different parts of the aggregate gradation. The calculation formula is shown in Equation (5). The nominal maximum particle size of the aggregate was 13.2 mm, and the standard $P_{C_P} = 13.2 \times 0.22 = 2.9$ mm was determined by the Bailey method, which was between 2.36 mm and 4.75 mm. Therefore, 2.9 mm was used as the virtual control sieve hole.

When calculating $P_{\mathrm{S}/2}$, $P_{\mathrm{S}/2} = 13.2 \times 0.5 = 6.6$ mm was obtained, which was between 4.75 mm and 9.5 mm. When the aggregate quantity was sufficient, the particle size of the mineral aggregate was uniformly and continuously changed. The pass rate of the virtual sieve hole calculated by the interpolation method was in line with that of the actual situation, and the theoretical formula of the interpolation is shown in Equations (6) and (7). From this, the R_{CA} values of design gradations 1 and 2 in different filling states could be obtained, as shown in Table 11:

$$R_{\mathrm{CA}} = \frac{P_{\mathrm{S}/2} - P_{C_P}}{100 - P_{\mathrm{S}/2}}, \tag{5}$$

where $P_{\mathrm{S}/2}$ = the half-sieve mesh pass rate (%), and P_{C_P} = the basic control screen pass rate (%). Equations (6) and (7) are

$$P_{2.9} = \frac{(4.75 - 2.9)}{(4.75 - 2.36)} P_{2.36} + \frac{(2.9 - 2.36)}{(4.75 - 2.36)} P_{4.75} = 0.77P_{2.36} + 0.23P_{4.75}, \tag{6}$$

$$P_{6.6} = \frac{(9.5 - 6.6)}{(9.5 - 4.75)} P_{4.75} + \frac{(6.6 - 4.75)}{(9.5 - 4.75)} P_{9.5} = 0.61P_{4.75} + 0.39P_{9.5}. \tag{7}$$

Table 11. R_{CA} value in aggregate filling state.

Project	Gradation 1		Gradation 2		
	Tamping State	Selected Tight State	Tamping State	Selected Tight State	Loose State
P2.9	31.29	35.85	25.49	28.86	30.58
P6.6	51.56	54.78	41.32	44.54	46.19
RCA	0.42	0.42	0.27	0.28	0.29
Specification limits	0.26–0.41				

It can be seen from Table 10 that the R_{CA} of gradation 1 exceeded the range required by the Bailey method, so it was discarded. The R_{CA} of gradation 2 was within the range required by the Bailey method. The aforementioned design aggregate gradation was compared to the commonly used SMA-13 specification gradation as a test grading, as shown in Figure 3.

It can be seen from Figure 5 that the 13.2-mm mesh pass rate was less than 90%, and the content of the nominal maximum particle size aggregate was increased relative to the Stone Matrix Asphalt (SMA) grade. This was advantageous for improving the compressive strength and stability of the skeleton structure. The coarse aggregate adopted the lower limit of the recommended value of the specification, and it was easy to form a real skeleton structure. The fine aggregate adopted the upper limit of the standard recommended value, so the gap ratio was small. In summary, the gradation in the selected state was used as the synthetic gradation of the final skeleton compaction result.

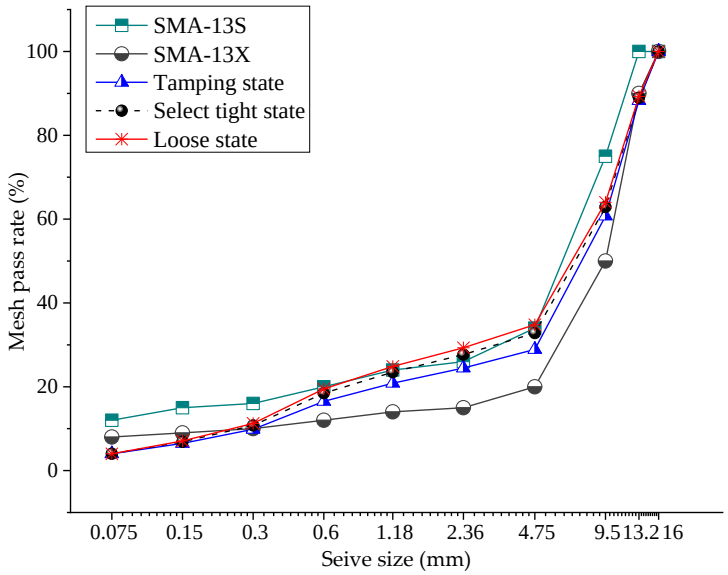

Figure 5. Comparison of test gradation and SMA gradation.

3.3. Type of Crumb Rubber Asphalt Mixture (CRTAM) Design and Sample Preparation

Compared to stone, rubber particles of the same quality are much larger. Inserting rubber of the same quality into a mixture will surely cause interference in the skeleton of the mixture, which will affect the structural stability of the mixture. Therefore, the incorporation of rubber particles generally uses the incorporation method, which uses an identical volume of rubber particles to replace a certain volume of stone. First of all, this paper used the equal volume replacement method to design a CRTAM with a different CRT content, and the optimum CRT content was determined according to the low-temperature index. Subsequently, the unequal volume replacement method was utilized to design CRTAMs with different substitution ratios and determine the amount of CRT.

3.3.1. Determination of Amount of CRT

Gradation 2 in the selected state was selected as the aggregate grading of the CRTAM design, and the CRT content was determined by the low-temperature index. The influence of the low temperature was mainly seen in the gradation, and the asphalt had less influence in the optimal range. Therefore, the uniform selection of the oil–stone ratio was 4.6%, and the same level was replaced by the same volume by substituting one volume of 1.5%, 2%, and 2.5% CRT instead of one volume of aggregate. The replacement results are listed in Table 12.

The number of times of rolling was selected as 28. The asphalt mixture was rolled and formed, and a low-temperature beam test was carried out. The results are shown in Figure 6.

Table 12. Gradation of mixtures under different CRT contents.

Content of CRT (%)	Mass Percentage (%) through Sieve Pore (mm)									
	16	**13.2**	**9.5**	**4.75**	**2.36**	**1.18**	**0.6**	**0.3**	**0.15**	**0.075**
1.5	100.00	88.57	61.61	30.46	25.16	20.83	15.64	9.74	6.77	4.14
2	100.00	88.44	61.18	29.68	24.32	19.94	14.70	9.40	6.74	4.19
2.5	100.00	88.31	60.75	28.90	23.48	19.05	13.75	9.06	6.70	4.23

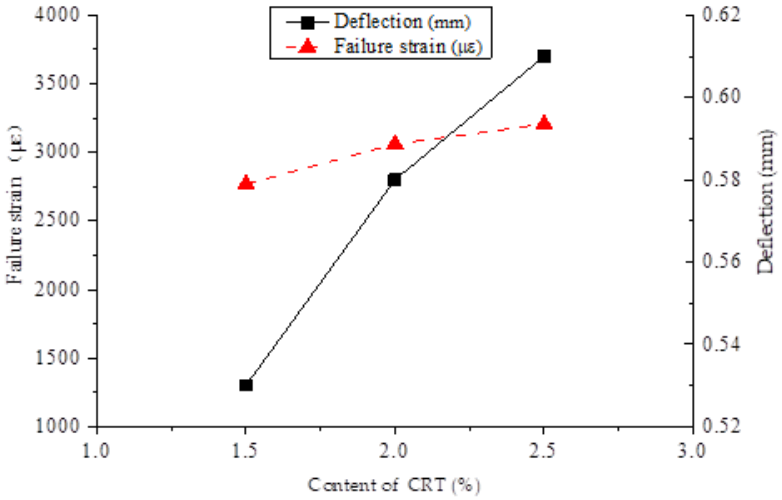

Figure 6. Results of low-temperature test.

It can be seen from Figure 6 that the low-temperature performance became better and better with an increase in the content, and it was necessary to meet the requirements of the "Technical Guidelines for Rubber Asphalt and Mixture Design and Construction" for a low-temperature bending test of CRAM of not less than 2800 με, so the rubber-blending amount was 2%.

3.3.2. Unequal Volume Replacement

If CRT accounted for 2% of the aggregate, the performance was better when using the same replacement method described in the previous section. Here, the volume of the rubber mixture of 2% was replaced by 0.5, 1, 1.5, 2, and 2.5 times the volume of the aggregate, and the substitution results are listed in Table 13. Due to the small proportion of aggregates with 2.36-mm and 1.18-mm particle sizes in the original grading, C and D were completely discontinuous at 1.18 mm and 2.36 mm, respectively. The gradations are listed in Table 13 below.

Table 13. Gradations of different substitution ratios.

Substitution Ratios	Mass Percentage (%) through Sieve Pore (mm)									
	16	**13.2**	**9.5**	**4.75**	**2.36**	**1.18**	**0.6**	**0.3**	**0.15**	**0.075**
0	100.00	88.94	62.90	32.80	27.68	23.49	18.48	10.77	6.88	4.00
0.5	100.00	88.69	62.05	31.24	26.00	21.72	16.59	10.09	6.81	4.09
1	100.00	88.44	61.18	29.68	24.33	19.94	14.70	9.40	6.74	4.19
1.5	100.00	88.18	60.32	28.12	22.65	18.16	12.81	8.72	6.66	4.28
2	100.00	87.92	59.46	26.56	20.97	16.39	10.91	8.03	6.59	4.37
2.5	100.00	87.67	58.60	25.00	19.29	14.61	9.02	7.35	6.52	4.46
C	100.00	88.47	61.28	29.86	24.52	24.52	19.29	11.24	7.18	4.17
D	100.00	88.35	60.90	29.17	29.17	24.76	19.48	11.35	7.25	4.22

3.4. Structural Determination

According to the gradation of the mixture in Table 13 and a CRT content of 2% (the mass of the aggregate), a Marshall test was carried out. The asphalt–aggregate ratio when the air void was 4% was the optimum asphalt–aggregate ratio. Through the Marshall test, the skeleton determination parameters of VCA_{DRC} (the coarse aggregate skeleton clearance rate in a tamping state), VCA_{mix} (the coarse aggregate skeleton clearance rate), VCA_{DLC} (the coarse aggregate skeleton clearance rate in a loose state), S (the skeleton stability), and the proportion of coarse aggregate under the optimum asphalt–aggregate ratio could be calculated. These are listed in Table 14.

Table 14. Parameters of structural determination under optimum asphalt–aggregate ratio.

Type	*OAC* (%)	VCA_{DRC} (%)	VCA_{mix} (%)	VCA_{DLC} (%)	S (%)	Proportion of Coarse Aggregate (%)
0	4.7	39.666	43.901	44.610	96.2	67.19
0.5	4.84		42.544		98.4	68.76
1	4.93		41.216		100.6	70.32
1.5	5.03		40.014		102.5	71.88
2	5.16		38.921		104.3	73.44
2.5	5.23		37.757		106.2	75.00
C	4.43		41.292		101.0	70.14
D	4.79		40.766		101.5	70.82

It can be seen from Table 14 that when the substitution ratio was 2.5, the $VCA_{mix} \leq VCA_{DRC}$ standard was suitable for the design of multiple gravel discontinuous components, such as the Stone Asphalt Concrete (SAC) and SMA. However, if S exceeded 105, this could cause aggregate fractures and increase the difficulty of onsite compaction.

4. Performance Evaluation

4.1. Analysis of High-Temperature Performance

Eight sets of gradation were used to shape the rutting plate, and they were tested through a rutting test at 60 °C. The rutting test was conducted with reference to the "Highway Engineering Asphalt and Asphalt Mixture Test Procedures" (JTG E20-2011). The results are shown in Figure 7. The dynamic stability and the relative deformation rate are shown in Figure 7a, and the ratio K of the dynamic stability to the relative deformation rate is shown in Figure 7b.

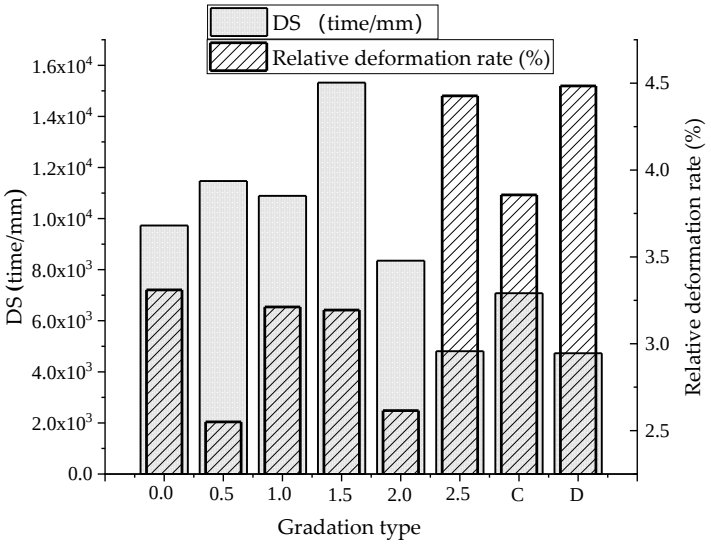

(**a**)

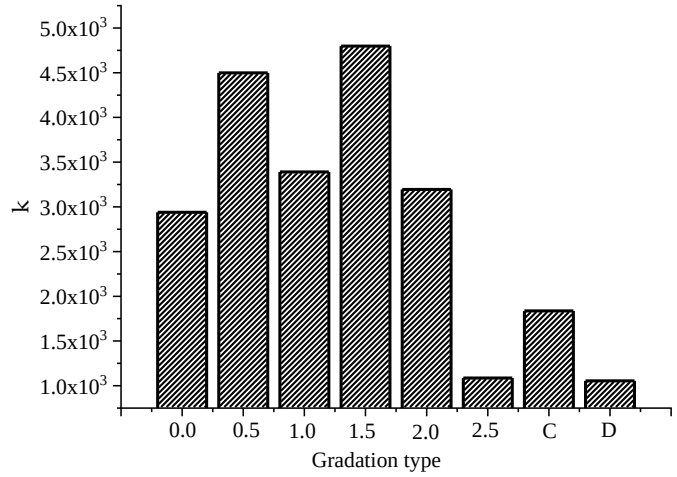

(**b**)

Figure 7. High-temperature test results for different mixture types. (**a**) Dynamic stability (DS) and relative deformation rate; (**b**) *K*.

As can be seen from Figure 7a, the dynamic stability (DS) first increased and then decreased as the substitution ratio increased and reached its maximum when the substitution ratio was 1.5. In the process of loading the asphalt mixture, no matter which structure was used, the load transfer path would always choose the large particle size [40]. When the substitution ratio was 1.5, the coarse aggregate was relatively large, the fine aggregate was enough to fill the skeleton, and a good embedded structure could be formed. Thus, the mixture exhibited better high-temperature performance. Since the CRT had higher elasticity, the detected value of the deformation rut depth may have been higher, so it is reasonable to assume that the actual high-temperature stability was better than the experimental value.

It can be seen from Figure 7a that the relative deformation rate and the trend of the DS were roughly opposite. Therefore, it was considered that the DS could not evaluate the influence of the CRT on the high-temperature performance of the asphalt mixture. The deformation rate was used as an auxiliary evaluation. To synthesize the two indicators, the high-temperature performance of the asphalt mixture was evaluated by the ratio *K* of the DS to the relative deformation rate. It can be seen

in Figure 7b that when the substitution ratio was 1.5 and 0.5, the performance was relatively good. From the perspective of comparative gradation, the gradation of 1.18 mm was higher than that of the 2.36-mm gradation.

4.2. Analysis of Low-Temperature Performance

In order to study the low-temperature performance of different grades of asphalt mixture and the effect of the substitution ratio on the low-temperature performance of the mixture, a low-temperature bending test was carried out at −10 °C. This experiment was conducted with reference to the "Highway Engineering Asphalt and Asphalt Mixture Test Procedures" (JTG E20-2011). The test results are shown in Figure 8.

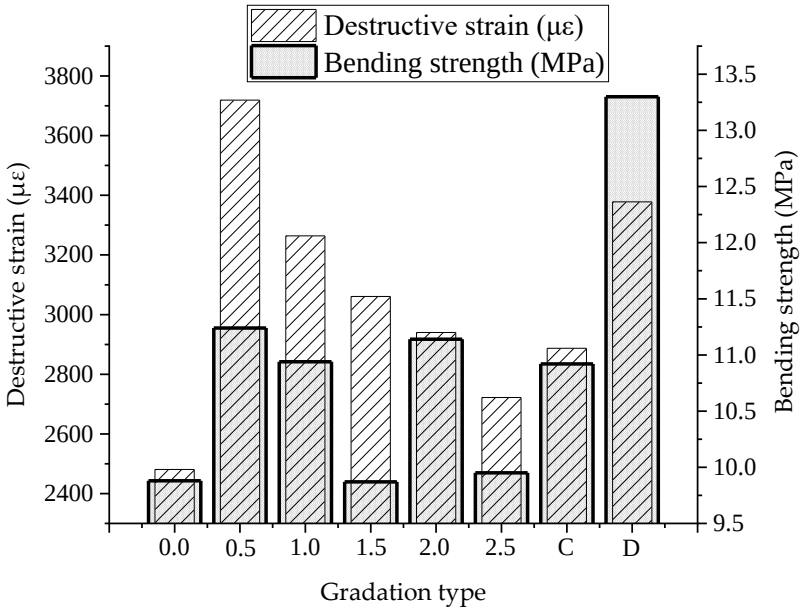

Figure 8. Low-temperature test results for different mixture types.

In practice, it is very difficult to achieve high strength and deformation ability at the same time, so it could not be determined if one indicator was better than the others. Thus, it was better to judge the low-temperature performance [41,42]. It can be seen in Figure 8 that the gradation order obtained by the two evaluation indexes was not completely consistent. The main reason was that the strain reflected the deformation ability, and the cracks appearing in the mixture were produced by a plurality of factors. Therefore, it was necessary to use the indexes of bending strain and bending strength for a comprehensive evaluation.

We considered that the index of the flexural strain energy density could simultaneously reflect the bending strain and the bending strength of the mixture. The function formula is shown as Equation (8) [43]:

$$W_f = \int_0^{\varepsilon_c} \sigma(\varepsilon) d\varepsilon, \tag{8}$$

where W_f = the flexural strain energy density (N·mm); ε_c = the strain value corresponding to peak stress; $\sigma(\varepsilon)$ = the stress component; and ε = the strain component.

The flexural strain energy density was calculated according to the stress–strain relationship, and this was used to evaluate the low-temperature crack resistance of the asphalt mixture. The test results are shown in Figure 9.

It can be seen in Figure 9 that the flexural strain energy density had a good correlation with the substitution ratio, and its value became larger and then smaller as the substitution ratio increased. In addition, there was a maximum value when the substitution ratio was 0.5. When the substitution

ratio was large, the fine aggregate did not completely fill the skeleton formed by the coarse aggregate in the asphalt mixture. Thus, there was a large gap, which made the binder ineffectively wrap on the aggregate surface, resulting in poor low-temperature performance. When the substitution ratio was lowered, the coarse aggregate skeleton void was reduced, and the mixture was more uniform and denser. At this time, the low-temperature performance of the asphalt mixture also increased. However, when the substitution ratio was further reduced, the rubber dimension interference with coarse aggregates resulted in a significant reduction in the low-temperature performance of the asphalt mixture.

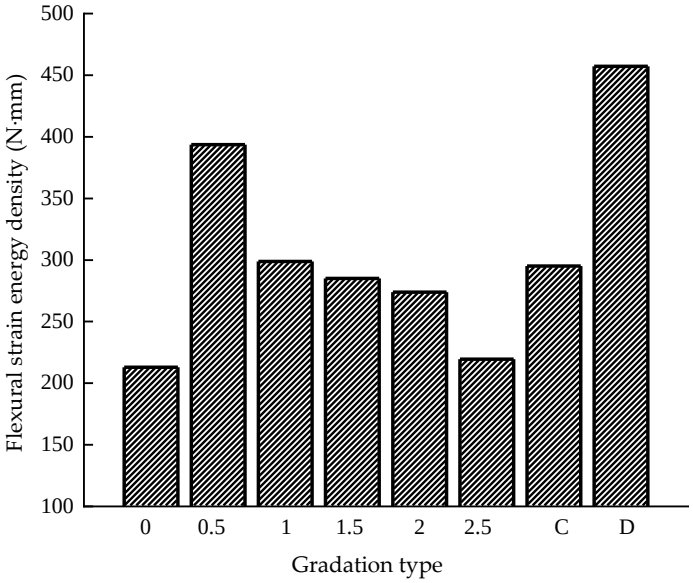

Figure 9. Flexural strain energy density for different mixture types.

4.3. Analysis of Water Stability

An immersion Marshall test and a freeze–thaw splitting test of different asphalt mixtures were carried out. They were conducted with reference to the "Highway Engineering Asphalt and Asphalt Mixture Test Procedures" (JTG E20-2011). The ratio of residual strength (TSR) and residual stability is shown in Figure 10. The freeze–thaw split was carried out 34 times, and the results are shown in Figure 11.

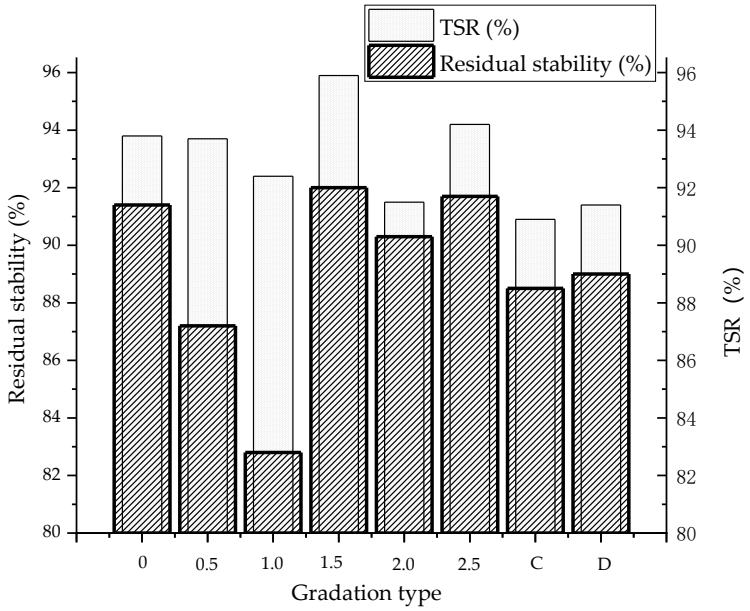

Figure 10. Water stability test results.

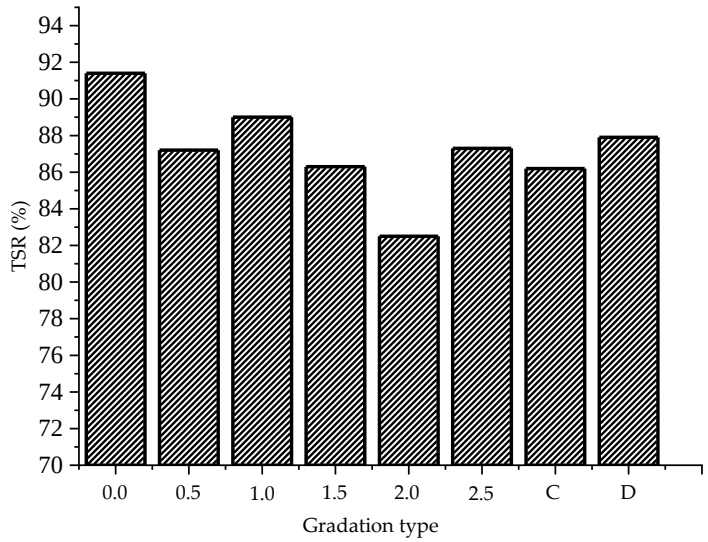

Figure 11. Freeze–thaw split test results (done 34 times).

It can be seen in Figure 10 that the residual stability of the eight gradation mixtures was greater than 85% in the immersion Marshall test, which satisfied the specification requirements. However, the residual stability and substitution ratio did not show obvious trends. By comparing Figures 10 and 11, it was found that for the same type of mixture, the failure load (after 50 compactions) and the damage load after freezing and thawing cycles were greater than 34 times those of the compaction test under the same conditions. According to the experimental data, the unfrozen and wrecked load of 34 compacted specimens was about 80% of the failure load of 50 compacted specimens under the same conditions. This was because the specimen compactness was better than 34 in 50 compaction cases.

The second case was real, so the former had a higher ability to withstand damage. This indicated that the compactness of the test piece had a great influence on the water stability effect. Compared to virgin asphalt, the addition of a rubber reticle in the test piece could significantly improve the water stability. China's regulations stipulate that the TSR value of the mixture should be greater than 80%, while the TSR of the matrix asphalt was 82% under the standard number of compactions, and the performance increased to 90% after the rubber powder was added. At 34 compactions, the mixture

TSR was 77%. After adding CRT, it basically reached 85% or higher. Thus, it could be found that CRT could significantly improve the water stability of the mixture.

5. Conclusions

In this paper, a gradation optimization design for a dry-process CRTAM with a skeleton dense structure was carried out, and the relevant road performance was analyzed. The main conclusions are as follows:

1. A skeletal intrusion compaction was used to optimize the grading of coarse aggregates and fine aggregates. Through the RCA test and a comparison of the standard grading, it was found that the gradation in the selected state was used as the synthetic gradation of the final skeleton compaction result;
2. When the volume by equal volume was replaced, the low-temperature performance was increasingly better with an increase in the dosage. Considering the economy and specifications, 2% CRT was selected. Marshall tests were carried out on six gradations of 2% CRT by unequal volume replacement and two common intermittent gradations. The results indicated that all of them met the requirement of $VCA_{mix} \leq VCA_{DLC}$. It can be concluded that these eight gradations had a dense skeleton structure;
3. For high-temperature stability, as an overall trend, DS first increased and then decreased with an increase in the substitution ratio and reached its maximum when the substitution ratio was 1.5. The integrated relative deformation rate introduced the K value, and when the substitution ratio was 1.5 and 0.5, the performance was relatively good. The water stability of the specimens was significantly improved by adding the CRT, and the water stability under 50 compaction conditions was better than that of the 34 compacted specimens under the same conditions;
4. The low-temperature performance was characterized by the flexural strain energy density, which could simultaneously exhibit the bending strain and the bending strength. The value first increased and then decreased with an increase in the substitution ratio, and the low-temperature performance was best when the substitution value was 0.5;
5. In terms of a comprehensive consideration of the various performances and economic benefits, the best CRT content of the proposed CRTAM was 2%, and the best substitution ratio was 0.5.

In previous research, crumb rubber activated by TOR has indeed been able to better improve the low-temperature performance of the mixture, and similar results were obtained in this study. Overall, this study successfully characterized an asphalt mixture with CRT and made a composition design of a CRTAM through the dry process. It is anticipated that this study will contribute to the further application of crumb rubber in asphalt pavement. In future research work, it is necessary to verify the durability of CRTAM. Fatigue properties of CRTAM could be further characterized to better understand the performance of the mixture under repeated loading. On the other hand, it can be verified whether the design method is universal for mixtures with other nominal maximum sizes of aggregates.

Author Contributions: Data curation, J.D., W.D., and Z.H.; formal analysis, J.D. and W.D.; methodology, F.M. and Z.F.; resources, F.M.; Writing—original draft, J.D.; Writing—review & editing, Z.F. and J.L. All authors have read and agreed to the published version of the manuscript.

Funding: This project were supported by the National Key R&D Program of China (NO. 2018YFB1600200) and the Special Fund for Basic Scientific Research of Central Colleges, Chang'an University (NO. 300102318208; 300102219513; 300102218509).

Conflicts of Interest: The authors declare no conflicts of interest.

References

1. Fu, Z.; Sun, Q.; Li, J. Preparation and performance characterization of asphalt sustained-release capsules. *Int. J. Pavement Res. Technol.* **2018**. [CrossRef]

2. Ma, F.; Zhang, C. Road Performance of Asphalt binder Modified with Natural Rock Asphalt. *Adv. Mater. Res.* **2013**, *634–638*, 2729–2732. [CrossRef]
3. Ahmadinia, E.; Zargar, M.; Karim, M.R.; Abdelaziz, M.; Shafigh, P. Using waste plastic bottles as additive for stone mastic asphalt. *Mater. Des.* **2011**, *32*, 4844–4849. [CrossRef]
4. Venudharan, V.; Biligiri, K.P.; Sousa, J.B.; Way, G.B. Asphalt-rubber gap-graded mixture design practices: A state-of-the-art research review and future perspective. Road Mater. *Pavement Des.* **2017**, *18*, 730–752. [CrossRef]
5. Moreno, F.; Sol, M.; Martin, J.; Perez, M.; Rubio, M.C. The effect of crumb rubber modifier on the resistance of asphalt mixes to plastic deformation. *Mater. Des.* **2013**, *47*, 274–280. [CrossRef]
6. Gogoi, R.; Biligiri, K.P.; Das, N.C. Performance prediction analyses of styrene-butadiene rubber and crumb rubber materials in asphalt road applications. *Mater. Struct.* **2016**, *49*, 3479–3493. [CrossRef]
7. Fontes, L.P.T.L.; Triches, G.; Pais, J.C.; Pereira, P.A.A. Evaluating permanent deformation in asphalt rubber mixtures. Constr. *Build. Mater.* **2010**, *24*, 1193–1200. [CrossRef]
8. Yu, X.; Leng, Z.; Wang, Y.; Lin, S. Characterization of the effect of foaming water content on the performance of foamed crumb rubber modified asphalt. *Constr. Build. Mater.* **2014**, *67*, 279–284. [CrossRef]
9. Bressi, S.; Fiorentini, N.; Huang, J.; Losa, M. Crumb Rubber Modifier in Road Asphalt Pavements: State of the Art and Statistics. *Coatings* **2019**, *9*, 384. [CrossRef]
10. Vazquez, V.F.; Luong, J.; Bueno, M.; Teran, F.; Paje, S.E. Assessment of an action against environmental noise: Acoustic durability of a pavement surface with crumb rubber. *Sci. Total Environ.* **2016**, *542*, 223–230. [CrossRef]
11. Licitra, G.; Moro, A.; Teti, L.; Del Pizzo, A.; Bianco, F. Modelling of acoustic ageing of rubberized pavements. *Appl. Acoust.* **2019**, *146*, 237–245. [CrossRef]
12. Girimath, S.; Singh, D.; Manthos, E.; Mampearachchi, W.K. Effects of reclaimed asphalt binder on rheological properties and cohesion energy of crumb rubber modified binder. Innov. *Infrastruct. Solut.* **2018**, *3*, 57. [CrossRef]
13. Praticò, F.G.; Vaiana, R.; Giunta, M.; Iuele, T.; Moro, A. Recycling PEMs back to TLPAs: Is that Possible Notwithstanding RAP Variability? *Appl. Mech. Mater.* **2012**, *253–255*, 376–384. [CrossRef]
14. Jiang, W.; Yuan, D.; Xu, S.; Hu, H.; Xiao, J.; Sha, A.; Huang, Y. Energy harvesting from asphalt pavement using thermoelectric technology. *Appl. Energy* **2017**, *205*, 941–950. [CrossRef]
15. Xiao, F.; Amirkhanian, S.N.; Shen, J.; Putman, B. Influences of crumb rubber size and type on reclaimed asphalt pavement (RAP) mixtures. *Constr. Build. Mater.* **2009**, *23*, 1028–1034. [CrossRef]
16. Jiang, W.; Xiao, J.; Yuan, D.; Lu, H.; Xu, S.; Huang, Y. Design and experiment of thermoelectric asphalt pavements with power-generation and temperature-reduction functions. *Energy Build.* **2018**, *169*, 39–47. [CrossRef]
17. Das, S.; Murthy, V.S.R.; Murty, G.S. Particulate size effect on the rheology of SiC-glass composites. *J. Mater. Sci.* **1999**, *34*, 1347–1352. [CrossRef]
18. Garcia-Morales, M.; Partal, P.; Navarro, F.J.; Martinez-Boza, F.J.; Gallegos, C. Processing, rheology, and storage stability of recycled EVA/LDPE modified bitumen. *Polym. Eng. Sci.* **2007**, *47*, 189–191. [CrossRef]
19. Säwe, M.; Klein, T.; Larem, D.; Mücke, M.; Pareigis, E. New Method for Producing Rubber-Modified Bitumen from Vulcanized Rubber: Germany. EP 20100162127, 14 December 2011.
20. Santagata, E.; Lanotte, M.; Baglieri, O.; Dalmazzo, D.; Zanetti, M.C. Analysis of bitumen–crumb rubber affinity for the formulation of rubberized dry mixtures. *Mater. Struct.* **2016**, *49*, 1947–1954. [CrossRef]
21. Yu, G.X.; Li, Z.-M.; Zhou, X.-L.; Li, C.-L. Crumb Rubber–Modified Asphalt: Microwave Treatment Effects. *Pet. Sci. Technol.* **2011**, *29*, 411–417. [CrossRef]
22. Xie, Z.X.; Shen, J.A. Effect of cross-linking agent on the properties of asphalt rubber. *Constr. Build. Mater.* **2014**, *67*, 234–238. [CrossRef]
23. Padhan, R.K.; Gupta, A.A.; Mohanta, C.S.; Badoni, R.P.; Bhatnagar, A.K. Performance improvement of a crumb rubber modified bitumen using polyoctenamer and cross linking agent. Road Mater. *Pavement Des.* **2017**, *18*, 999–1006. [CrossRef]
24. Liang, M.; Ren, S.S.; Fan, W.Y.; Wang, H.; Cui, W.Y.; Zhao, P.H. Characterization of fume composition and rheological properties of asphalt with crumb rubber activated by microwave and TOR. *Constr. Build. Mater.* **2017**, *154*, 310–322. [CrossRef]

25. Kashif, M.; Kim, S.J.; Chang, Y.W. Shape memory polymer blends of syndiotactic 1,2-polybutadiene and trans-polyoctenamer. *Polym. Bull.* **2016**, *74*, 1–10. [CrossRef]
26. Liang, M.; Xin, X.; Fan, W.; Ren, S.; Shi, J.; Luo, H. Thermo-stability and aging performance of modified asphalt with crumb rubber activated by microwave and TOR. *Mater. Des.* **2017**, *127*, 84–96. [CrossRef]
27. Liu, H.Y.; Chen, Z.J.; Wang, W.; Wang, H.N.; Hao, P.W. Investigation of the rheological modification mechanism of crumb rubber modified asphalt (CRMA) containing TOR additive. *Constr. Build. Mater.* **2014**, *67*, 225–233. [CrossRef]
28. Ng Puga, K.L.N.; Williams, R.C. Low temperature performance of laboratory produced asphalt rubber (AR) mixes containing polyoctenamer. *Constr. Build. Mater.* **2016**, *112*, 1046–1053. [CrossRef]
29. Kang, A.H.; Zhang, Q.; Li, P. Research on the Influences of the Molding Processes of TOR Asphalt Rubber Mixtures upon the Pavement Performance. *Adv. Mater. Res.* **2012**, *535–537*, 1819–1824. [CrossRef]
30. Lo Presti, D.; Fecarotti, C.; Clare, A.T.; Airey, G. Toward more realistic viscosity measurements of tyre rubber-bitumen blends. *Constr. Build. Mater.* **2014**, *67*, 270–278. [CrossRef]
31. Pereira, P.; Pais, J. Main flexible pavement and mix design methods in Europe and challenges for the development of an European method. *J. Traffic Transp. Eng. (Engl. Ed.)* **2017**, *4*, 8–38. [CrossRef]
32. Xie, Z.X.; Shen, J.N. Performance of porous European mix (PEM) pavements added with crumb rubbers in dry process. *Int. J. Pavement Eng.* **2016**, *17*, 637–646. [CrossRef]
33. Farouk, A.I.B.; Hassan, N.A.; Mahmud, M.Z.H.; Mirza, J.; Jaya, R.P.; Hainin, M.R.; Yaacob, H.; Yusoff, N.I.M. Effects of mixture design variables on rubber-bitumen interaction: Properties of dry mixed rubberized asphalt mixture. *Mater. Struct.* **2017**, 50. [CrossRef]
34. Li, Z.; Li, C. Improvement of properties of styrene-butadiene-styrene-modified bitumen by grafted eucommia ulmoides gum. *Road Mater. Pavement Des.* **2013**, *14*, 404–414. [CrossRef]
35. Lopez-Moro, F.J.; Moro, M.C.; Hernandez-Olivares, F.; Witoszek-Schultz, B.; Alonso-Fernandez, M. Microscopic analysis of the interaction between crumb rubber and bitumen in asphalt mixtures using the dry process. *Constr. Build. Mater.* **2013**, *48*, 691–699. [CrossRef]
36. Gawel, I.; Stepkowski, R.; Czechowski, F. Molecular Interactions between Rubber and Asphalt. *Ind. Eng. Chem. Res.* **2006**, *45*, 3044–3049. [CrossRef]
37. Kedarisetty, S.; Saha, G.; Biligiri, K.P.; Sousa, J.B. Reacted and Activated Rubber (RAR)-Modified Dense-Graded Asphalt Mixtures: Design and Performance Evaluation. *J. Test. Eval.* **2018**, *46*, 2511–2520. [CrossRef]
38. Mahmoud, E.; Masad, E.; Nazarian, S. Discrete Element Analysis of the Influences of Aggregate Properties and Internal Structure on Fracture in Asphalt Mixtures. *J. Mater. Civil Eng.* **2010**, *22*, 10–20. [CrossRef]
39. Mahmoud, E.; Masad, E. A Probabilistic Model for Predicting the Resistance of Aggregates in Asphalt Mixes to Fracture. Road Mater. *Pavement Des.* **2010**, *11*, 335–360.
40. Liu, H. *Study on Volume Parameter Properties and Gradation Mix Design Method of Asphalt Mixture*; Chang'an University: Xi'an, China, 2007.
41. Liu, J.; Zhao, S.; Li, L.; Li, P.; Saboundjian, S. Low temperature cracking analysis of asphalt binders and mixtures. *Cold Reg. Sci. Technol.* **2017**, *141*, 78–85. [CrossRef]
42. Zhang, Z.; Zhao, Z.; Zhang, W. Effect of aggregate gradation on performance of asphalt mix at low temperature. *J. Chang. Univ. (Nat. Sci. Ed.)* **2005**, *25*, 1–5.
43. Ge, Z.; Huang, X.; Xu, G. Evaluation of asphalt-mixture's low-temperature anti-cracking performance by curvature strain energy method. *J. Southeast Univ. (Nat. Sci. Ed.)* **2002**, *32*, 653–655.